



## Bioactive and degradable hydrogel based on human platelet-rich plasma fibrin matrix combined with oxidized alginate in a diabetic mice wound healing model



Itxaso Garcia-Orue<sup>a,b,c,1</sup>, Edorta Santos-Vizcaino<sup>a,b,c,1</sup>, Pello Sanchez<sup>d</sup>, Francisco Borja Gutierrez<sup>e</sup>, Jose Javier Aguirre<sup>e,f</sup>, Rosa Maria Hernandez<sup>a,b,c,\*</sup>, Manoli Igartua<sup>a,b,c,\*</sup>

<sup>a</sup> NanoBioCel Research Group, Laboratory of Pharmaceutics, School of Pharmacy, University of the Basque Country (UPV-EHU), Vitoria-Gasteiz, Spain

<sup>b</sup> Biomedical Research Networking Centre in Bioengineering, Biomaterials and Nanomedicine (CIBER-BBN), Institute of Health Carlos III, Madrid, Spain

<sup>c</sup> Bioaraba, NanoBioCel Research Group, Vitoria-Gasteiz, Spain

<sup>d</sup> Arthroscopic Surgery Unit, Hospital Vithas San José, Vitoria-Gasteiz, Spain

<sup>e</sup> Bioaraba Health Research Institute, Osakidetza Basque Health Service, Araba University Hospital, Pathological Anatomy Service, Vitoria-Gasteiz, Spain

<sup>f</sup> Biokeralty Reseach Institute, Vitoria-Gasteiz, Spain

### ARTICLE INFO

#### Keywords:

Platelet Rich Plasma  
Hydrogel  
Chronic wound

### ABSTRACT

In the present study we developed an injectable, bioactive and degradable hydrogel composed of alginate at 2.5% oxidation degree and calcium-activated platelet rich plasma (PRP) for wound healing applications (PRP-HG-2.5%). The alginate gives mechanical support to the hydrogel while the activated PRP provides growth factors that enhance wound healing and fibrin which creates an adequate microenvironment for cell migration and proliferation. The rheological and mechanical properties of the hydrogel were characterized. Further characterization revealed that PRP-HG-2.5% showed a faster hydrolytic degradation rate than unmodified alginate and a similar platelet derived growth factor (PDGF-BB) release profile. *In vitro* efficacy studies, carried out in human fibroblasts and keratinocytes, showed that PRP-HG-2.5% was not cytotoxic and that it was able to promote cell adhesion and proliferation. Thereafter, in an *in vivo* full thickness wound healing study conducted in diabetic mice, no differences were found among PRP-HG-2.5% and its counterpart without PRP, likely due to the xenogeneic origin of the PRP. This hypothesis was validated *in vitro*, since a cytotoxic effect was observed after human PRP application to mouse fibroblasts. Therefore, PRP-HG-2.5% might be a promising strategy for chronic wound treatment, although its effectiveness should be evaluated in a more reliable preclinical model.

### 1. Introduction

Ageing is one of the most challenging social and economic issues in the XXI century. Old people are more susceptible to develop disabilities or multimorbidity complications [1], such as, chronic wounds. An affection that usually appears associated with diabetes, venous insufficiency and obesity [2]. The estimated costs associated to wound healing are approximately 3% of the worldwide health care expenditure. Solely in the USA, more than 25 billion dollars are expended yearly in chronic wounds [3,4].

Due to underlying diseases or changes in the regulation of the process, chronic wounds are not always able to progress through the highly organized wound healing process, and thus, they remain open for long periods,

usually longer than a year [5]. Consequently, they are more susceptible to infections and to frequent relapses, which has a great impact in the patient life quality [6].

Since the efficacy of current treatments cannot be guaranteed, researchers are making a big effort to develop new treatments able to accelerate wound healing. A new approach that is gaining importance is the administration of exogenous growth factors (GFs), since they are key molecules in the regulation of the healing process and usually are downregulated in chronic wounds [7]. In order to administer multiple GFs and chemokines in a physiological proportion, the use of activated platelet rich plasma (PRP) has been proposed [8]. PRP is an autologous concentrate of platelets in a small volume of plasma, which, once activated, releases a great amount of GFs and chemokines that have an important role in wound healing, such as, Platelet Derived Growth Factor (PDGF), Transforming Growth Factor -  $\beta$  (TGF- $\beta$ ), Vascular Endothelial Growth Factor (VEGF), Granulocyte Macrophage Colony Stimulating Factor (GM-CSF), Fibroblast Growth Factor (FGF) family, Epithelial Growth Factor (EGF) family, the interleukin (IL) family and the Tumor Necrosis Factor-alpha

\* Corresponding authors at: Laboratory of Pharmaceutics, University of the Basque Country, School of Pharmacy, Paseo de la Universidad 7, 01006 Vitoria-Gasteiz, Spain.

E-mail addresses: [rosa.hernandez@ehu.es](mailto:rosa.hernandez@ehu.es) (R.M. Hernandez), [manoli.igartua@ehu.es](mailto:manoli.igartua@ehu.es) (M. Igartua).

<sup>1</sup> These two authors contributed equally to this work.

<sup>2</sup> R.M. Hernandez and M. Igartua equally share credit for senior authorship.

(TNF- $\alpha$ ) [9]. Lastly, the activated PRP (actPRP) creates a fibrin clot that forms a provisional matrix, along with fibronectin and other ECM proteins present in actPRP. That provisional matrix contains cell binding sites, which provide an adequate microenvironment for cell growth, favoring the migration of fibroblasts and keratinocytes onto the wound [10–12]. Overall, the effects of actPRP on wound healing are the following: (1) revascularization through the induction of migration, proliferation and differentiation of endothelial cells in new blood vessels; (2) the promotion of migration, proliferation, and (3) protein synthesis of dermal fibroblasts; and modulation of the inflammatory process [10,13].

However, actPRP presents some limitations for its topical use, such as, poor mechanical properties, difficult handling or the shrinkage of the fibrin clot that leads to an early release and loss of GF rich serum. Some strategies able to overcome these issues in clinical practice and accelerate chronic wound closure, were platelet rich lipotransfect, a mixture of PRP and autologous fat graft [14] and the use of a bio-functionalized scaffold composed of platelet-rich plasma (PRP) and hyaluronic acid [9,15].

In the current study, we decided to incorporate actPRP into hydrogels, which are hydrophilic lattices of a hydrated polymeric network. Hydrogels present a beneficial combination of high water content, flexibility, softness and excellent biocompatibility, which makes them suitable for wound healing. Furthermore, due to their high water content, hydrogels cool the wound surface, which has a pain alleviating effect [16–18]. This is reinforced by their permeability to oxygen and water vapour without water leakage [19].

In that regard, numerous research groups have developed hydrogels containing PRP from human or rodent origin. In those studies, several hydrogel-forming polymers were used, such as, chitosan and silk fibroin [20], gelatin [21], oxidized dextran and modified hyaluronic acid [22], poly-*n*-acetyl glucosamine [23], and poly(*d,l*-lactide)-poly(ethylene glycol)-poly(*d,l*-lactide) [24]. In the current study, we chose alginate as the hydrogel-forming polymer, since it has been extensively used for wound healing purposes [25,26]. A limitation of alginate hydrogels however, is their low and unpredictable degradation *in vivo* through dissociation of the ionic crosslinking. One approach to improve this issue is the oxidation of alginate, obtaining alginate dialdehyde (ADA), which presents a faster degradation making it more attractive for regenerative processes [27].

Accordingly, the aim of this study was to develop an injectable bioactive and degradable hydrogel composed of activated PRP and oxidized alginate to obtain a sustained release of GFs and provide a provisional fibrin matrix for cell proliferation and migration. We used calcium sulphate is used to crosslink alginate, initiate platelet degranulation and activate the clotting process of the fibrin.

We controlled the degradation rate of alginate by oxidizing it at different percentages. We characterized the obtained hydrogels for their suitability in wound healing, and we chose the most adequate to undergo *in vitro* studies in human fibroblasts and keratinocytes. Finally, we analyzed hydrogel's efficacy *in vivo*, in a full-thickness excisional wound study carried out in *db/db* mice. Due to the unexpected results obtained *in vivo*, we assessed the effect of xenogeneic human PRP administration on mice fibroblasts *in vitro*.

## 2. Materials and methods

### 2.1. PRP obtaining and characterization

We obtained PRP from healthy volunteers according to the protocol approved by the Institutional Ethical Committee for Research Involving Human beings of the University of the Basque Country (UPV/EHU), procedure number M10/2019/080. We collected peripheral blood into 9 ml tubes containing 3.8% of sodium citrate (Vacuette, Greiner Bio-one, Switzerland). Afterwards, we centrifuged the blood at 480g for 10 min, and carefully collected the PRP from the bottom 2 ml of the plasma fraction, those just above the leukocyte buffy coat.

We characterized the PRP determining the level of the following cytokines: bFGF, EGF, IGF-1, PDGF-AA, PDGF-AB, PDGF-BB, VEGF and TGF- $\beta$ .

Briefly, we activated the PRP using a saturated calcium sulphate dissolution (Sigma-Aldrich, MO, USA). Then, we drained and discarded the fibrin clot that was formed upon activation, and we collected the serum containing GFs and cytokines released after platelet degranulation. Thereafter, we conducted a multiplex ELISA assay on that serum, following the manufacturer's instructions (Tebubio, France).

### 2.2. Alginate oxidation and characterization

We oxidized ultrapure LVM sodium alginate (Pronova, Sweden) following the procedure described by Bouhadir et al. [28]. We dissolved sodium alginate at 1% (w/v) in Milli-Q water and made it reacted with different amounts of sodium periodate (Sigma-Aldrich, MO, USA) to obtain different oxidation degrees. We maintained the reaction under mechanical stirring for 17 h at room temperature and in the dark. Then, we stopped the reaction adding an equimolar quantity of ethylene glycol (Sigma-Aldrich, MO, USA) for 30 min. We dialyzed the resulting solution (Spectra/Por 6, MWCO 3.5 kDa; Repligen, MA, USA) in Milli-Q water for 3 days with 2–3 water changes per day. Then to eliminate any impurities, we added 0.5 g of activated charcoal (Sigma-Aldrich, MO, USA) per gram of alginate. Finally, the solution was sterile-filtered (0.22  $\mu$ m; Sterycup, Merck, NJ, USA) and lyophilized (Lyobeta 15, Telstar, Spain).

We dissolved oxidized alginate in PBS at different concentrations *i.e.*, 1, 2 and 4 and 6% (w/v), and we measured the viscosity on an AR1000 rheometer (TA instruments, DE, United States) with 40 mm diameter flat plate geometry at 20 °C. We used the viscosity of unmodified alginate at a concentration of 1.5% (w/v) as the control viscosity, due to its adequate mechanical properties.

### 2.3. Hydrogel preparation

We dissolved alginates at different oxidation degrees in PBS at the chosen concentrations and we mixed them with PRP in a ratio 1:1. Thereafter, we crosslinked the mixtures with 1.22 M CaSO<sub>4</sub>·2H<sub>2</sub>O (Sigma-Aldrich, MO, USA) in Milli-Q water through two LuerLock syringes (BD Syringe, NJ, USA) connected with a Fluid Dispensing Connector (Braun, Germany). We mixed both syringes for 10 s and then we allowed the crosslinking reaction to occur for 1 min before extruding the cross-linked hydrogel. Thus, we obtained hydrogels composed by actPRP and unmodified, 2.5% oxidized or 5% oxidized alginate (PRP-HG, PRP-HG-2.5% or PRP-HG-5% respectively). As controls, we also prepared hydrogels containing only alginate with different oxidation degrees following the same procedure. We named these formulations HG, HG-2.5% and HG-5%, respectively.

For some experiments, we needed hydrogels with the same geometry and volume, in order to be able to establish differences among groups. For that purpose, we moulded hydrogels between two glass plates with a 1.5 mm spacer (except for the strain and frequency sweeps where we used a 0.5 mm spacer) and we allowed them to crosslink for 15 min at 37 °C. Then, we obtained discs of 6, 10, or 40 mm in diameter using a circular punch.

For *in vitro* experiments containing cells, we dissolved alginate in cell culture medium without calcium (DMEM 21068–028, Gibco®, MA, USA) and sterile filtered (Stericup, Millipore, MA, USA). Furthermore, we prepared those hydrogels under aseptic conditions.

### 2.4. Hydrogel characterization

#### 2.4.1. Rheological properties

We measured rheological properties of all hydrogels by means of the AR1000 rheometer (TA instruments, DE, USA) equipped with a 40 mm diameter flat plate geometry at 37 °C and the gap set at 500  $\mu$ m. Firstly, we conducted an oscillatory time sweep shear study to obtain the gelation time, using the results obtained for the storage modulus ( $G'$ ) and the loss modulus ( $G''$ ). Briefly, we mixed the PRP-alginate mixture and the calcium sulphate onto the rheometer plate and the conditions were set at 0.5% strain and 1 Hz angular frequency. We expressed  $G'$  and  $G''$  moduli

measurements as a function of time and we considered that gelation was complete when the value of the  $G'$  modulus reached a plateau.

In addition, we also carried out strain and frequency sweep studies. For these experiments, we prepared hydrogels discs of 40 mm in diameter and 0.5 mm in height. For the strain sweep study, we set the angular frequency at 1 Hz and the strain from 0.5 to 20%. Once we defined the linear viscoelastic region (LVE) of the hydrogels, we conducted a frequency sweep study setting the strain at 1% and the angular frequency in a range of 0.5 to 40%.

#### 2.4.2. Mechanical properties

We tested the effect of compression on the hydrogels using a TA.XT.PlusC texture analyzer (Stable Micro Systems, UK). We compressed hydrogel discs of 10 mm in diameter using a probe of 20 mm in diameter with a displacement rate of 0.1 mm/s, to assess the compressive stress at 60% strain.

#### 2.4.3. Hydrolytic degradation

First, we immersed hydrogel discs of 10 mm in diameter in DPBS with calcium and magnesium (BE17-513F, Lonza, Switzerland) at 37 °C. At selected time points (0 h, 1 h, 4 h, 8 h, 24 h, 48 h, 4 days and 7 days); we collected the hydrogels, washed with Milli-Q water and lyophilized them. Finally, we weighed the dried discs and we calculated the percentage of the remaining weight using the following equation (Eq. (1)):

$$\text{Remaining weight (\%)} = \frac{\text{Dry weight at selected time points}}{\text{Dry weight at time 0}} \times 100 \quad (1)$$

#### 2.4.4. Water vapour transmission rate

We determined the Water Vapour Transmission Rate (WVTR) of the hydrogel following a modified procedure of the method described by Li et al. [29]. Using a 10 mm diameter hydrogel disc, we completely sealed the mouth of a vessel filled with silica gel desiccant, so water vapour could only enter to the vessel through the hydrogel disc. We weighed the assembly in the beginning of the study and then placed in a chamber at  $30 \pm 2$  °C with a constant relative humidity of 75%. After 24 h, we weighed again the assembly and we calculated the WVTR using the following equation (Eq. (2)):

$$\text{WVTR} = \frac{M_1 - M_0}{A \times T} \quad (2)$$

where  $M_0$  is the weight of the assembly at the beginning of the assay,  $M_1$  is its weight after the incubation time,  $T$  is the exposure time (1 day) and  $A$  is the exposure area ( $0.79 \text{ cm}^2$ ).

#### 2.4.5. PDGF-BB release

To study the release of GFs and cytokines from the hydrogel, we used PDGF-BB as a model GF. Firstly, we prepared PRP-HG, PRP-HG-2.5% and PRP-HG-5% hydrogels and cut them into discs of 10 mm in diameter. We transferred those discs to 1.5 ml centrifuge tubes with filters (Spin X centrifuge tube filter, Costar, VA, USA) containing 500  $\mu\text{l}$  DPBS with calcium and magnesium. We incubated the discs at 37 °C and at selected time points; we collected the supernatants centrifuging the tubes at 1000 G for 10 min. Then, we replaced the collected supernatants with 500  $\mu\text{l}$  of fresh PBS. We measured the PDGF-BB concentration on the supernatants using a commercially available ELISA kit for human PDGF-BB (human PDGF-BB ELISA development kit, Peprotech, NJ, USA). We performed the assay following the manufacturer's instructions.

We expressed the results as the released percentage from the total PDGF-BB content in the discs. We determined the total content of PDGF-BB breaking down the hydrogel discs with 0.1 M EDTA and quantifying their PDGF-BB content using the same ELISA kit.

### 2.5. In vitro cell culture studies in human cells

#### 2.5.1. Cell culture

The cell lines used in this study were HaCaT keratinocytes and Human Dermal Fibroblasts (HDF) (ATCC, VA, USA). We cultured the first one on Dulbecco's modified Eagle's medium (DMEM) (41965-039, Gibco®, MA, USA) supplemented with 10% (v/v) foetal bovine serum (FBS) and 1% (v/v) penicillin-streptomycin. We cultured primary human dermal fibroblasts isolated from adult skin (HDF, ATCC®, VA, USA) on complete medium that consisted on fibroblast basal medium (PCS-201-030, ATCC®, VA, USA) supplemented with fibroblast growth kit-low serum (PCS-201-041, ATCC®, VA, USA) and 1% (v/v) penicillin-streptomycin. We incubated cell lines in a humidified incubator at 37 °C with a 5%  $\text{CO}_2$  atmosphere and we performed cell passages every 3–5 days depending on the cell line.

#### 2.5.2. Cell viability studies

We assessed indirect cytotoxicity incubating cells with the conditioned medium of PRP-HG, PRP-HG-2.5% and HG-2.5% hydrogels.

We incubated hydrogel discs of 10 mm in diameter with 0.5 ml of culture medium for 24 h at 37 °C, to obtain the conditioned medium. In addition, we also incubated medium with actPRP in the same volume as in the PRP-HG-2.5%. Finally, as negative and positive controls, we used culture medium and culture medium with 10% (v/v) DMSO respectively.

In parallel, we seeded cells on 96 well plates at a density of 5000 cells/well and 10,000 cells/well for HDF and HaCaT cells, respectively. We incubated the cells overnight to allow cell attachment and then, we replaced the culture medium by the conditioned medium of the hydrogels. After 24 h of incubation, we assessed cell viability through a CCK-8 colorimetric assay (Cell Counting Kit-8, Sigma-Aldrich, MO, USA). Briefly, we added 10  $\mu\text{l}$  of the CCK-8 reagent to the cells and incubated for 4 h. We read the absorbance of the wells at 450 nm, using 650 nm as reference wavelength (Plate Reader Infinite M200, Tecan, Switzerland) and its value was directly proportional to the number of living cells in each well. We gave the results as the percentage of living cells comparing to the control.

For direct cytotoxicity studies, we seeded cells on 24 well plates at a density of 35,000 cells/well and 70,000 cells/well for HDF and HaCaT cells, respectively. We incubated cells overnight to allow cell adhesion, and then we added PRP-HG, PRP-HG-2.5% and HG-2.5% hydrogel discs of 6 mm in diameter to the wells in transwell culture inserts, to ease their removal. In addition, we also added actPRP in the same volume as in the PRP-HG-2.5% to the wells. Finally, as negative and positive controls, we used culture medium and culture medium with 10% (v/v) DMSO respectively. We incubated cells for 48 h and then as in the indirect cytotoxicity assay, we assessed cell viability through the CCK-8 colorimetric assay.

#### 2.5.3. Cell proliferation

We seeded HaCaT and HDF cells on 96 well plates at a density of 2000 cells/well. We incubated HDF cells overnight. We incubated HaCaT cells firstly for 6 h in complete medium to allow cell adhesion and then in starving medium (medium with 0.2% FBS) overnight.

Using the same procedure described in the previous 2.5.2. section, we obtained conditioned medium for the following formulations: PRP-HG, PRP-HG-2.5%, HG-2.5% and PRP. To reduce background proliferation signals, we kept FBS at 0.4% and 2% for HDF and HaCaT respectively. We added BrdU to the cells in the conditioned medium, and after a 24 h incubation, we performed a BrdU ELISA assay following the manufacturer instructions (Cell Proliferation Kit, BioTrak™ ELISA Kit, Cytiva, MA, USA). We read the absorbance of the wells at 450 nm (Plate Reader Infinite M200, Tecan, Switzerland), and its value was directly proportional to the incorporated BrdU and thus to cell proliferation.

#### 2.5.4. Cell adhesion

We placed discs of 10 mm in diameter of PRP-HG, PRP-HG-2.5% and HG-2.5% in 24 well plates and we seeded 250,000 HDF cells on top of them. We allowed cells to adhere and spread in the hydrogels for 24 h.

Afterwards, we fixed them with 3.7% formaldehyde (Panreac, Spain) permeabilized and stained with Alexa Fluor 488-labelled Phalloidin for F-actin (Thermo Fisher Scientific, MA, USA) and DAPI for the nuclei (Thermo Fisher Scientific, MA, USA) following the manufacturer's instructions. We acquired fluorescent micrographs by means of a confocal fluorescence microscope (LSM800, Zeiss, Germany).

## 2.6. *In vivo* wound healing study

### 2.6.1. Animals

For this study, we used 8-week-old 32 male *db/db* (BKS.Cg-m + / + Leprdb/J) mice (Janvier laboratories, France). We conducted all the experiments following the protocols approved by the Institutional Ethical Committee for Animal Experimentation of the University of the Basque Country (Procedure number: M20/2019/258). We housed the mice individually with a light-dark cycle of 12 h, and we gave them *ad libitum* access to standard rodent chow and water.

### 2.6.2. Wound healing assay

We performed the wound healing assay modifying slightly the procedure described by Michaels et al. [30]. We anesthetized mice with isoflurane (Isoflo®, Esteve, Spain) and removed their dorsal hair. Then, we sutured two silicone rings (1 cm diameter) on each side of the midline using a 3-0 nylon suture (Aragó, Spain) to avoid wound contraction and make reepithelization the main healing mechanism, as it is in human wound healing. Thereafter, in the middle of each splint, we created a full thickness wound extending through the *panniculus carnosus*, using an 8 mm in diameter punch biopsy tool (Acu-Punch, Acuderm, FL, USA). We cleaned wounds using saline, we applied treatments topically and we covered the wounds with one layer of petrolatum gauze (Tegaderm®, 3M, MN, USA) and two layers of adhesive.

We divided mice into 4 groups ( $n = 8$ ) depending on the treatment they received: (i) untreated control, (ii) 100  $\mu$ l of actPRP, (iii) 100  $\mu$ l HG-2.5% and (iv) 100  $\mu$ l of PRP-HG-2.5%.

On days 4, 8, and 11, we removed the hydrogels and applied new treatments. We sacrificed half of the mice on day 8 and the remaining ones on day 15, by means of CO<sub>2</sub> inhalation.

### 2.6.3. Evaluation of wound healing

We evaluated the macroscopic effectiveness of the treatments determining the wound closure percentage through all the experiment. For that purpose, on days 1, 4, 8, 11 and 15 we photographed wounds next to a ruler for scaling using a digital camera (Ixus 190, Canon, Japan). We assessed the area of each wound using an image analysis programme (ImageJ®, Biophotonics Facility, University of McMaster, Canada). Finally, we calculated the wound closure percentage using the following equation (Eq. (3)):

$$\text{Wound closure (\%)} = \frac{\text{Final wound area (px}^2\text{)}}{\text{Initial wound area (px}^2\text{)}} \times 100 \quad (3)$$

### 2.6.4. Histological analysis of wound healing

After mice sacrifice, we excised the wound and surrounding tissue (about 1 × 1 cm) and fixed in 3.7% formaldehyde (Panreac, Spain). After 24 h of fixing, we bisected the biopsies, embedded them in paraffin and sectioned in layers of 5  $\mu$ m thickness. We stained those slices with haematoxylin-eosin (H&E) to evaluate their progress through wound healing process, regarding reepithelization and resolution of the inflammatory phases.

To assess the reepithelization process, we used the scale described by Sinha et al. [31]. According to that scale, we rated semi-quantitatively wounds from 0 to 4; where 0 means that only wound edges are reepithelized; 1 means that less than half of the wound is reepithelized; 2 means that more than half of the wound is covered in new epithelia; 3 means that the entire wound is covered in new epithelia with irregular

thickness; and 4 means that the entire wound is reepithelized with normal thickness.

We determined the resolution of the inflammatory process and wound maturity in accordance with the scale established by Cotran et al. [32]. We assigned to each wound a semi-quantitative number according to the following criteria: 0, no inflammation; 1, acute inflammation that comprises the formation of the fibrin clot and of the pyogenic membrane and the migration of leucocytes and polymorphonuclear neutrophils to the wound; 2, diffuse acute inflammation, which consists in the formation of granulation tissue and angiogenesis and in the almost complete disappearance of the pyogenic membrane; 3, proliferation, this phase consists in fibroblast proliferation and 4, resolution and healing, in which the chronic inflammation has disappeared, although occasionally round cells can be observed.

## 2.7. *In vitro* cell culture studies in murine cells

### 2.7.1. Cell culture

In this study, we used the L929 murine fibroblast cell line (ATCC, VA, USA), in order to compare the results with those obtained with human fibroblasts (HDF). We cultured cells on Eagle's Minimum Essential Medium (EMEM; ATCC, VA, USA) supplemented with 10% (v/v) inactivated Horse Serum and 1% (v/v) penicillin-streptomycin, and we incubated them at 37 °C in a humidified incubator with a 5% CO<sub>2</sub> atmosphere. We performed cell passages every 2–3 days depending on cell confluence.

### 2.7.2. Cell viability studies

We performed cell viability studies using the same procedure described in Section 2.5.2 for the indirect and the direct cytotoxicity assays, with the following modifications: we used L929 murine cells, and we seeded them at 5000 cells/well and 35000 cells/well density for indirect and direct assays, respectively.

### 2.7.3. Cell proliferation

We performed a cell proliferation study following the same procedure as in Section 2.5.3. but using the L929 murine cell line. We seeded cells at 2000 cells/well density and we starved them overnight (medium without FBS). To reduce the background proliferation stimuli, the conditioned medium included only a 2% FBS concentration.

## 2.8. Statistical analysis

We performed each experiment in triplicate in three independent assays. We expressed the results as the mean  $\pm$  standard deviation (SD). Following the results from Shapiro-Wilks normality test, we analyzed results through one-way ANOVA test for multiple comparisons, since they showed a normal distribution. Based on the Levene test for the homogeneity of variances, we applied Bonferroni or Tamhane post-hoc. We performed all the statistical tests using SPSS 22.0.01 (SPSS®, INC., IL, USA). Finally, we created graphs using GraphPad Prism (v. 5.01, GraphPad Software, Inc., CA, USA).

## 3. Results

### 3.1. Hydrogel characterization

The hydrogels developed in this study were composed of actPRP and unmodified alginate or alginate at 3 different oxidation degrees, 2.5%, 5% and 10%. We analyzed the viscosity of each oxidation degree at different concentrations and we showed those with a Newtonian rheological behavior in Fig. 1A.

The viscosity of alginate is related to the post-gelled mechanical properties, and thus we chose alginate dissolutions with a viscosity in the range of 0.3–0.5 Pa·s, since the viscosity of the unmodified alginate at 1.5% (w/v) is in that range (0.33  $\pm$  0.007 Pa·s). We selected the viscosity of unmodified alginate at 1.5% (w/v) as the model one, since that concentration is



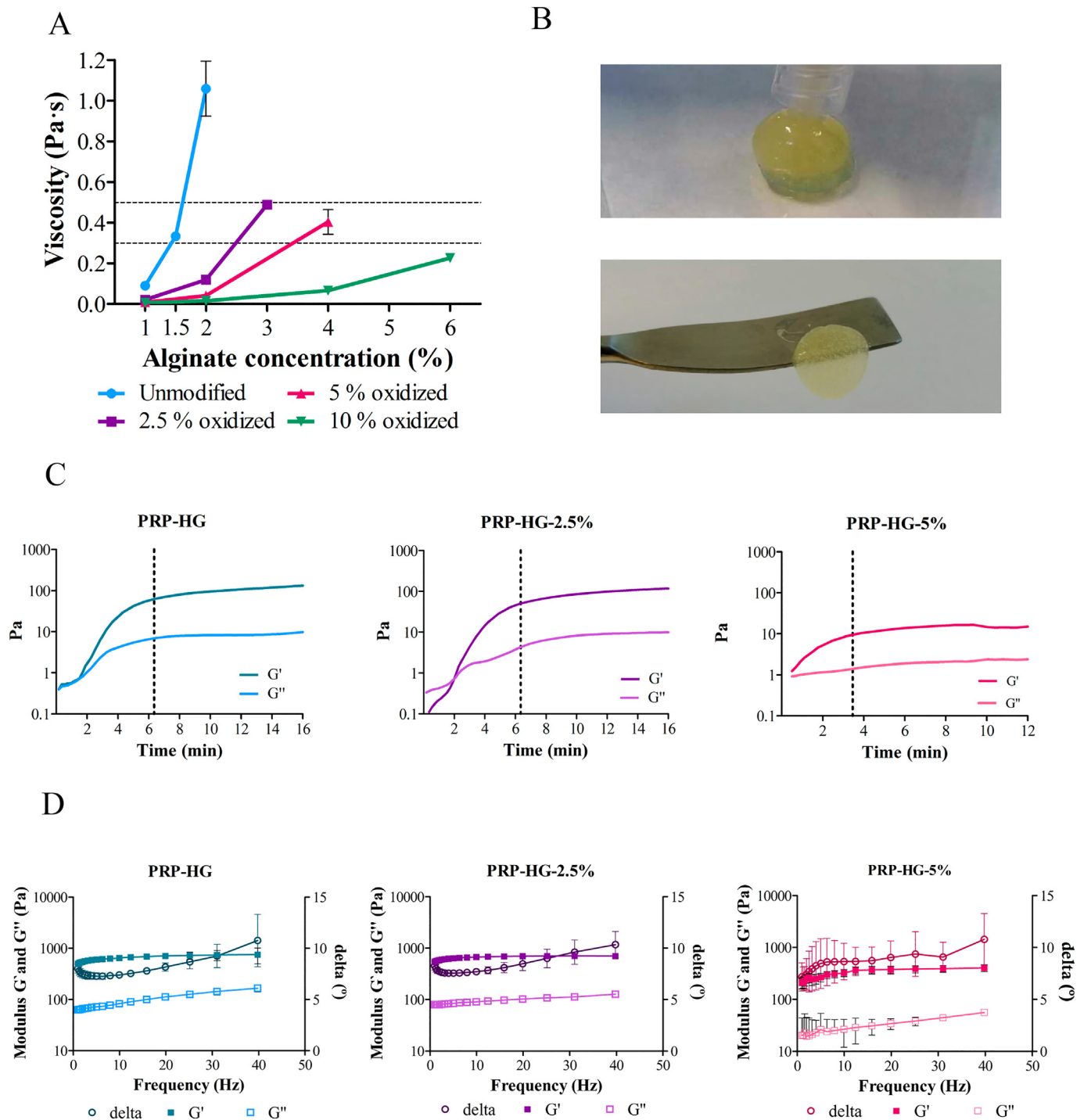


**Fig. 1.** (A) Alginate viscosity. The viscosity of alginates with different oxidation degrees at a range of concentrations are represented. We gave in terms of the mean viscosity (Pa·s)  $\pm$  SD. (B) Macroscopic images of PRP-HG-2.5 hydrogel, at the preparation (up) and after a mature disc was obtained (down). (C) Gelation time. A time sweep test of hydrogels prepared with alginates with different oxidation degrees. The gelation time is indicated when both  $G'$  and  $G''$  stabilize reaching a plateau. (D) Frequency sweep test performed in hydrogels prepared with alginates with different oxidation degrees.

commonly used for hydrogels and microcapsules formulations due to its optimal rheological and mechanical properties [33]. Therefore, the chosen concentrations to develop the composite hydrogels were 3% (w/v) for 2.5% oxidized alginate and 4% (w/v) for 5% oxidized alginate, which had  $0.49 \pm 0.006$  Pa·s and  $0.4 \pm 0.06$  Pa·s viscosity, respectively. Regarding 10% oxidized alginate, its viscosity was very low, in fact even with the highest concentration that showed a Newtonian behavior (6%), it did not reach the minimum viscosity of 0.3 Pa·s. Therefore, we discarded this oxidation degree and no further experiments were carried out with it.

Thereafter, we prepared composite hydrogels mixing PRP, oxidized alginate at the chosen concentrations and calcium sulphate. Macroscopic images of the appearance of the hydrogel can be observed in Fig. 1B. For the characterization of the hydrogels, we carried out rheological studies. Firstly, a time sweep test determined that the gelation time was similar in PRP-HG and PRP-HG-2.5% — about 6 min until complete gelation — as indicated by the stabilization of the storage modulus ( $G'$ ) and the loss modulus ( $G''$ ) into a plateau. The PRP-HG-5% hydrogel, however, presented a lower gelation time, about 3.5 min until complete gelation (Fig. 1C).

Then, we conducted a strain sweep test to define the LVE region of the hydrogels (Supplementary Fig. S1). Using the LVE region, we chose a strain value for the frequency sweep, which was conducted to assess the bulk viscoelastic properties. The results of the frequency sweep test showed a very similar behavior for PRP-HG and PRP-HG-2.5% (Fig. 1D). The storage modulus ( $G'$ ) ranged from 498 to 753 Pa and from 546 to 702 Pa for PRP-HG and PRP-HG-2.5%, respectively. Loss modulus ( $G''$ ) was lower in both cases, showing the gel-like nature of the developed hydrogels. Their  $G''$  values and behavior were similar, ranging between 63 and 166 Pa for PRP-HG and between 80 and 128 Pa for PRG-HG-2.5%. On the other hand, PRP-HG-5% hydrogels presented lower values both in  $G'$  and  $G''$ , since they varied between 208 and 403 Pa and between 20 and 56 Pa for  $G'$  and  $G''$  respectively. Hence, the lower  $G'$  values evidence the lower stiffness of the PRP-HG-5% formulation.

We also observed this lesser stiffness of the PRP-HG-5% in the compression study, where we determined the compressive stress at 60% strain

(Fig. 2A). Both PRP-HG and PRP-HG-2.5% showed significantly higher ( $p < 0.001^{***}$ ) values than PRP-HG-5%, highlighting the lower stiffness of the PRP-HG-5% hydrogel.

As expected, the oxidation degree conditioned the hydrolytic degradation rate of the hydrogels, both in hydrogels with and without PRP (Fig. 2B and Supplementary Fig. S2A). PRP-HG-5% hydrogels presented the faster degradation rate, with a remaining weight of  $27 \pm 4.2\%$  of their initial weight after 24 h. PRP-HG and PRP-HG-2.5% degraded significantly slower, showing remaining weights of  $49.3 \pm 7.8\%$  and  $47.7 \pm 5.1\%$ , respectively, after 24 h. At day 7, PRP-HG-5% and PRP-HG-2.5% presented similar percentages of the remaining weight —  $22.9 \pm 7.3\%$  and  $26 \pm 9$ , respectively — while PRP-HG maintained the same  $49.2 \pm 16\%$  of the first 24 h. Regarding their counterparts without PRP, HG hydrogel maintained a remaining weight above 88% during the whole study, statistically higher values than PRP-HG in all time points (Supplementary Fig. S2B). Regarding, HG-2.5%, it showed a slower hydrolytic degradation than PRP-

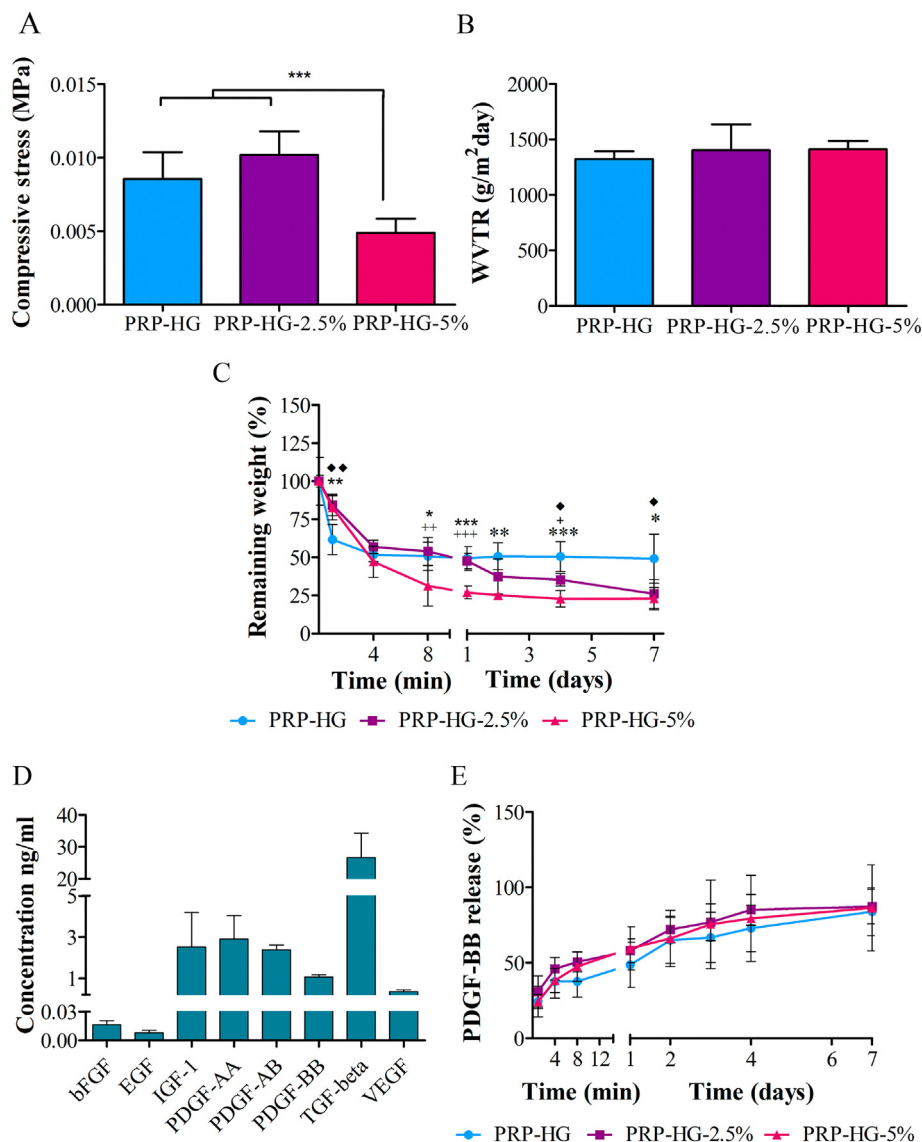


**Fig. 2.** (A) Mechanical strength. A compression test to assess the compressive stress at 60% strain.  $^{***} p < 0.001$  comparing PRP-HG and PRP-HG-2.5% with PRP-HG-5% We expressed results as mean stress (MPa)  $\pm$  SD. (B) Water vapour transmission rate (WVTR). We gave results in terms of the mean viscosity (Pa-s)  $\pm$  SD. (C) Hydrolytic degradation study. The percentage of remaining dry weight of hydrogels at different time points regarding it dry weight at time 0. \*  $p < 0.05$ ,  $^{**} p < 0.01$  and  $^{***} p < 0.001$  comparing PRP-HG and PRP-HG-5%. +  $p < 0.05$ , ++  $p < 0.01$  and +++  $p < 0.001$  comparing PRP-HG-2.5 and PRP-HG-5%. □  $p < 0.05$  and □□  $p < 0.01$  comparing PRP-HG and PRP-HG-2.5%. (D) PRP's GF content. Results of an ELISA multiplex with the concentration (ng/ml) of GFs present in the PRP: bFGF, EGF, IGF-1, PDGF-AA, PDGF-AB, PDGF-BB, TGF- $\beta$  and VEGF. We expressed results as mean concentration  $\pm$  SD. (E) PDGF-BB release profile. PDGF-BB cumulative *in vitro* release profile from PRP-HG, PRP-HG-2.5% and PRP-5%. We performed the assay in triplicate and we gave the results in terms of the mean  $\pm$  SD of the cumulative percentage of rhEGF released over time.

HG-2.5%, since it reached a remaining weight of  $53 \pm 12.3\%$  on day 7 as observed in Supplementary Fig. S2C. Finally, HG-5% showed a statistically significant slower degradation than PRP-HG-5% until day 4, but it was completely degraded for day 7 (Supplementary Fig. S2D).

We determined the permeability of the hydrogels to allow water vapour to enter or exit the wound, through the WVTR. As shown in Fig. 2C, it was very similar in the 3 formulations, being,  $1322.1 \pm 70.8 \text{ g/m}^2\text{day}$ ,  $1404.8 \pm 231.8 \text{ g/m}^2\text{day}$  and  $1410.2 \pm 77.1 \text{ g/m}^2\text{day}$ , for PRP-HG, PRP-HG-2.5% and PRP-HG-5% respectively.

We analyzed the content of GFs directly in the actPRP using a multiplex ELISA (Fig. 2D). TGF- $\beta$  was the most abundant GF with a concentration of  $26.7 \pm 7.7 \text{ ng/ml}$ . Next, with a concentration between 1 and 3 ng/ml were IGF-1, PDGF-AA, PDGF-AB and PDGF-BB. Finally, with the lowest concentration among the analyzed GFs, there were VEGF, bFGF and EGF, with  $350 \pm 77.8 \text{ pg/ml}$ ,  $16.4 \pm 4.3 \text{ pg/ml}$  and  $7.85 \pm 2.6 \text{ pg/ml}$ , respectively.

To analyze the release profile of factors from the hydrogels, we chose PDGF-BB as a representative GF. All the formulations presented a similar profile, with an initial burst release phase, where about 50% of PDGF-BB was released in the first 24 h and a posterior sustained release phase that reached a plateau around 85% on day 7 (Fig. 2E).

Although we performed the characterization using both PRP-HG-2.5% and PRP-HG-5%, we conducted the *in vitro* and *in vivo* studies using only the PRP-HG-2.5% hydrogel, since it presented more suitable mechanical properties and degradation profile. In fact, PRP-HG-5% degradation was about 75% in 24 h, which is excessive for wound healing treatment, since dressings are maintained in the wound at least for 2–3 days.

### 3.2. *In vitro* cell culture studies in human cells

We analyzed the cytocompatibility of the developed hydrogel in the two main human cell types that are present in skin and have a pivotal role in wound healing: fibroblasts (HDF) and keratinocytes (HaCaT). Every formulation tested showed no cytotoxicity, since their viability was above 70% in comparison to the negative control, both in direct and indirect tests (Fig. 3A, B).

Thereafter, we performed a proliferation test to determine whether the GFs present in the PRP were able to promote the proliferation of fibroblasts and keratinocytes (Fig. 3C). The actPRP itself and the formulations containing it — PRP-HG and PRP-HG-2.5% — were able to significantly enhance the BrdU uptake in comparison to the control group and to the formulation without actPRP — HG-2.5%—. However, no differences were observed among groups containing actPRP. In addition, HG-2.5% formulation did not enhance proliferation in comparison to the control group.

Due to the beneficial properties that actPRP confers on the formulation; it creates an adequate microenvironment for cell adhesion. Besides, of cytokines and GFs, the clotted fibrin of actPRP has an important role in cell adhesion, since it acts as a natural matrix for cell migration and adhesion due to its cell-binding sites. Accordingly, fibroblasts seeded on top of the hydrogels were able to adhere on top of PRP-HG and PRP-HG-2.5% hydrogels, showing an elongated spindle-shaped morphology, typical of fibroblasts (Fig. 3D). The cells seeded on top of HG-2.5%, on the contrary, were not able to adhere, due to the lack of fibrin present in the alginate. Hence, only a few poorly adhered cells could be observed occasionally on the entire surface of the hydrogel.

### 3.3. *In vivo* wound healing study

We evaluated the efficacy of PRP-HG-2.5% calculating the wound closure in a full thickness splinted wound healing assay, carried out in *db/db* mice. We divided animals in 4 groups; the first one did not receive any treatment, as it was the untreated control, we treated the second and third groups with actPRP and HG-2.5% respectively, as they are the components of the selected hydrogel; and finally, the fourth group received PRP-HG-2.5% as treatment. We measured the wounds areas ( $\text{px}^2$ ) from

photographs taken on days 1, 4, 8 and 15 post wounding, and we calculated the wound closure as the percentage of the initial area.

As observed graphically (Fig. 4A) and in macroscopic images (Fig. 4B), from day 8 until the end of the study, groups treated with HG-2.5% and PRP-HG-2.5% showed a statistically significant enhancement in wound closure compared to the control, with non-statistical differences between them. Wound area reduction values obtained with actPRP alone only reached statistical significance against the control during the first week of treatment (days 4 and 8), and no differences were observed from that time point onwards.

Results obtained from histological analysis for reepithelization grade (Fig. 4C) and resolution of the inflammatory process (Fig. 4D) revealed no differences on day 8. However, on day 15, the group treated with HG-2.5% achieved a significantly higher reepithelization grade than the control, with score values of  $3.3 \pm 1.2$ , and  $1.5 \pm 1$  respectively. In regards to the resolution of inflammation, both HG-2.5% and PRP-HG-2.5% presented more mature wounds than the control group, with score values of  $3.1 \pm 0.4$ ,  $2.7 \pm 0.5$ , and  $0.9 \pm 0.8$ .

### 3.4. *In vitro* cell culture studies in murine cells

Given the inconsistency between *in vitro* and *in vivo* studies, we tried to elucidate whether the xenogeneic administration of human PRP in mice was responsible of the lack of therapeutic effect *in vivo*. For such aim, we next analyzed the effect of the formulations in a murine fibroblast cell line (L929) *in vitro*, to compare the results with the previously obtained in human fibroblasts.

First, we conducted a new cell viability study in murine cells. All the hydrogel-based formulations — PRP-HG, PRP-HG-2.5% and HG-2.5% — showed no cytotoxicity (Fig. 5AB). However, the actPRP alone caused a dramatic drop in the viability, with values that matched those of the positive controls (DMSO at 10% (v/v) in both direct and indirect assays:  $4.6 \pm 0.8\%$  and  $30.3 \pm 2.8\%$  respectively).

In line with the results observed in the biocompatibility assays, proliferation also decreased in a significant way upon administration of xenogeneic actPRP, probably due to cell death. In addition, none of the hydrogel-based formulations containing actPRP — PRP-HG and PRP-HG-2.5% — enhanced cell proliferation as compared to the formulation without it — HG-2.5% — (Fig. 5C).

## 4. Discussion

The aim of the current study was to develop a bioactive and degradable hydrogel composed of actPRP and oxidized alginate for the treatment of chronic wounds. Thus, we intended to find a synergistic effect between the properties of the components: the structural function of cross-linked alginate, the ECM-like biofunctionalization of fibrin and the pro-regenerative effect of the GF derived from platelets releasates. This hydrogel is intended for autologous use in clinical practice, since the use of autologous PRP alone or combined with biomaterials have shown a beneficial outcome in reconstructive surgery [14]. However, in the current study, we used a pool of different donors to reduce the inter-individual variability and obtain comparable results. Indeed multiple factors from patients affect PRP's composition, such as, sex, age, blood pressure, height, diet, stress, physiological status and pharmacological treatments [34].

PRP is a platelet concentrate in a small volume of plasma, which contains several GFs capable of stimulating important cellular processes for wound healing, such as mitogenesis, cell differentiation, chemotaxis and angiogenesis [9]. Therefore, we first characterized the actPRP analyzing the concentration of some of its main GFs, concretely: TGF- $\beta$ , PDGF-AA, PDGF-AB, PDGF-BB, VEGF, IGF-I, EGF and bFGF (Fig. 2D) [35]. Given the lack of standardization in obtaining PRP and the great interindividual variability, the GFs levels differ considerably between studies, making it difficult to exert direct comparisons. However, the levels of GFs obtained in the present study are within the ranges observed in the literature [36].

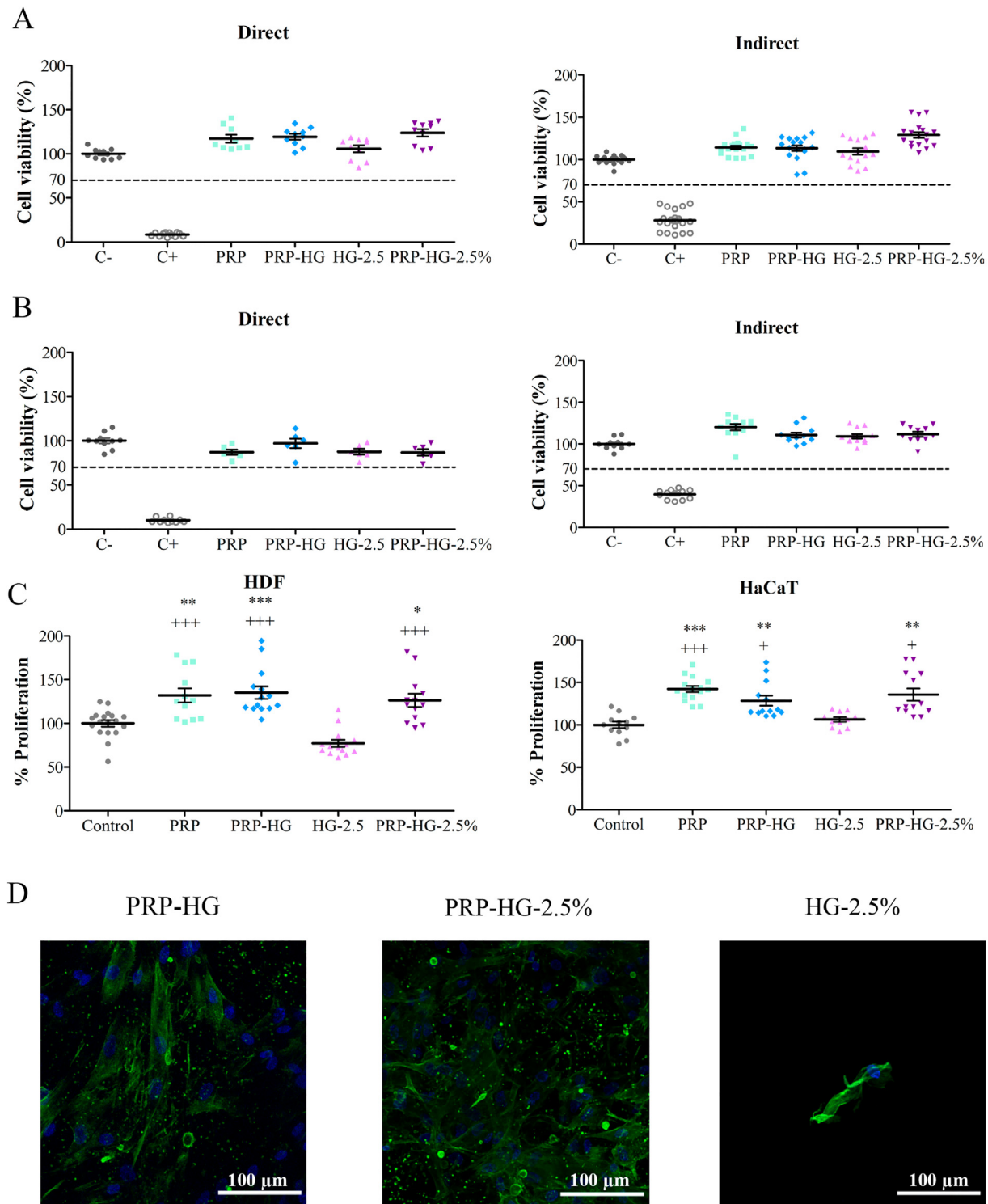


**Fig. 3.** *In vitro* assays in human cell lines. (A) Cytotoxicity assay on HDF cells, indirect and extraction assays. We gave results as mean  $\pm$  SD percentage of viability regarding control. (B) Cytotoxicity assay on HaCaT cells, indirect and extraction assays. We gave results as mean  $\pm$  SD percentage of viability regarding control. (C) Proliferation assay on HDF and HaCaT cells. Cell proliferation results are given as mean  $\pm$  SD percentage of proliferation regarding control. \*  $p < 0.05$ , \*\* $p < 0.01$  and \*\*\* $p < 0.001$  comparing with control. +  $p < 0.05$ , ++  $p < 0.01$  and +++  $p < 0.001$  comparing with HG-2.5%. (D) Confocal images of fibroblast adhesion onto the surface of the developed hydrogels. Nuclei are stained in blue and F-actin in green. The scale bars indicates 100  $\mu$ m.

On the other hand, we added alginate to the formulation because of its capacity to form hydrogels and reticulate, providing moisture and mechanical integrity to the composite system. In addition, it can actively participate in wound healing [37]. In the present study, we used a derivative of alginate obtained from its oxidation. During the oxidation process, the hydroxyl groups of the second and third carbon positions of each guluronate unit of alginate

chain are oxidized, forming aldehydes and leading to the breakage of the carbon-carbon bond. Those aldehydes react with adjacent hydroxyl groups of unoxidized residues in the chain, forming cyclic hemiacetals and thus altering the spatial conformation to an open-chain adduct [27,28].

Unlike unmodified alginate — which degrades very slowly and unpredictably due to dissociation of the ionic crosslinking — the obtained



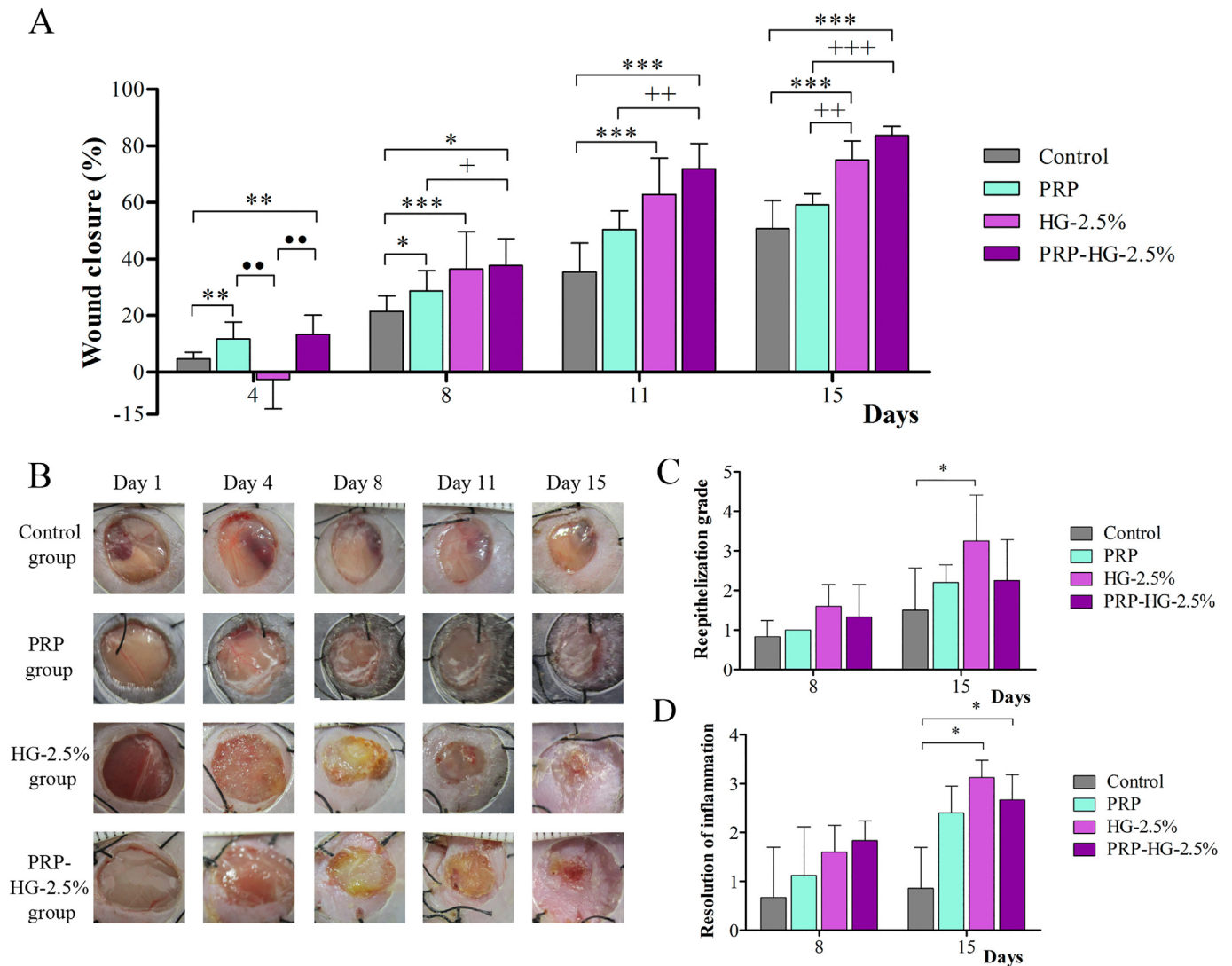


**Fig. 4.** *In vivo* wound healing assay in db/db mice. (A) Wound closure represented as the percentage of wound area reduction of the initial area on days 4, 8, 11 and 15 after wound induction. \*  $p < 0.05$ , \*\*  $p < 0.01$  and \*\*\*  $p < 0.001$  in comparison to control group. ●●  $p < 0.01$  in comparison to HG-2.5%. And +  $p < 0.05$ , ++  $p < 0.01$  and +++  $p < 0.001$  in comparison to PRP group. (B) Representative wound images of each groups on days 1, 4, 8, 11 and 15. (C) Reepithelization grade of the wounds on days 8 and 15. \*  $p < 0.05$  in comparison to control group. (D) Grade of resolution of the inflammatory process and maturation of the wound on days 8 and 15. \*  $p < 0.05$  in comparison to control group.

oxidized alginate is degradable and its degradation rate relies on its oxidation degree [38]. Therefore, we aimed to design a formulation that degrades in a few days, so it disappears from the wound for the next dressing change. This way, we avoid damage to the newly formed tissue associated to the removal of formulations that promote cell adhesion and migration.

Upon oxidation, the molecular weight of alginate decreases, which is attributed to the breakage of the main chain during oxidation [39]. Alginate's molecular weight is closely related to its rheological properties in the pre-gelled solution and mechanical properties in the post-gelled solution. Therefore, an increase in oxidation degree will lead to a lower molecular weight and thus to a lower pre-gelled viscosity and post-gelled rigidity

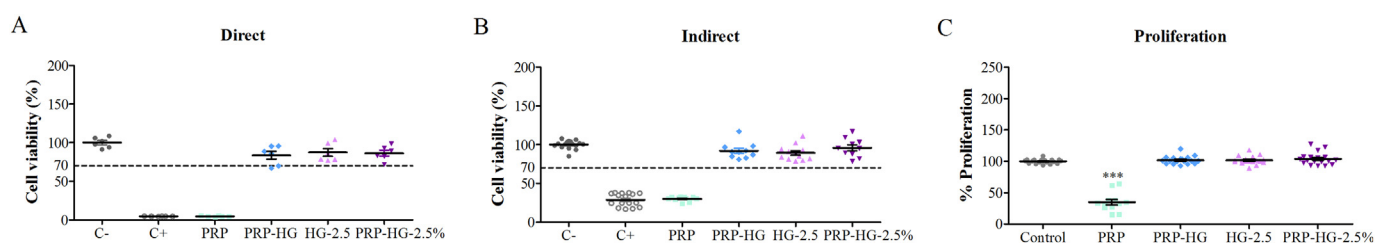


**Fig. 5.** *In vitro* assays in a murine cell line. (A) Indirect cytotoxicity assay. (B) Extraction cytotoxicity assay. We gave results as mean  $\pm$  SD percentage of viability regarding control. (C) Proliferation assay. We gave cell proliferation results as mean  $\pm$  SD percentage of proliferation regarding control. \*\*\*  $p < 0.001$  comparing every group with the group that received PRP.

[39]. In the current study, to obtain similar properties with all the formulations, we used alginate solutions with different concentration, since the stiffness of hydrogels and viscosity of solutions can be enhanced increasing their concentration [33]. To achieve that goal, we assessed the viscosity of oxidized alginates at different concentrations, to select those that were in the same viscosity range than a 1.5% (w/v) dissolution of unmodified alginate —0.3–0.5 Pa·s— (Fig. 1A). We chose that dissolution as the optimal one, due to its adequate mechanical properties, endorsed by its extensive use in hydrogels and cell microcapsules preparation [40–45]. Thereby, we selected the appropriate concentration for alginates oxidized at 2.5% and 5%. We removed the alginate oxidized at 10% from the study, due to a very low viscosity in the tested concentrations.

Regarding mechanical properties, PRP-HG-5% presented inferior mechanical properties than PRP-HG and PRP-HG-2.5%, as observed in frequency sweep (Fig. 1D) and compression tests (Fig. 2A). As previously reported, the worsening of the mechanical properties could be due to the lower molecular weight of the oxidized alginate and to the inability of open-chain adducts to form ionic bridges with ionic crosslinking molecules [28]. However, no differences in mechanical properties were observed between PRP-HG and PRP-HG-2.5%.

As expected, we observed a faster degradation rate as the oxidation degree increased, possibly since the oxidation might confer a free rotation to the  $\beta$ -glycosidic linkage of alginate, making the hemiacetal group susceptible to hydrolysis (Fig. 2B) [28]. Nevertheless, overall a fast degradation occurred in the beginning of the study with the hydrogels containing PRP in comparison to their counterparts without PRP (Supplementary Fig. S2). This could be explained due to the plasmin-mediated enzymatic degradation of the fibrin, as a result of the plasminogen activation [46].

Another crucial aspect to consider in the development of topical formulations is the value of WVTR to maintain an adequate moisture balance: an excessively high WVTR leads to a rapid drying of the wound — increasing the chances of scar formation — while an excessively low WVTR accumulates exudates [47]. The developed hydrogels presented a value around 1500 g/m<sup>2</sup>day (Fig. 2C), which lies within the range reported for commercial dressings (426–2047 g/m<sup>2</sup>day) [48].

We assessed the *in vitro* release of factors from the hydrogels using PDGF-BB as a representative GF. All the analyzed hydrogels (PRP-HG, PRP-HG-2.5% and PRP-HG-5%) showed a similar release profile. To ensure a complete GF release, an exogenous triggering factor is needed, in this study, we used calcium sulphate, since calcium presented a dual action, as PRP activator and alginate cross-linker [49]. The release profile presented an initial burst release where about 50% of the GF was released in the first 24 h. That fast release of GFs has been hypothesized to accelerate the recruitment of incoming progenitors cells, and thus to speed the beginning of the regenerative process [50]. Subsequently, a sustained release phase occurs that reached a release about 85% on day 7.

Therefore, based on the obtained results, we selected the hydrogel composed of actPRP and alginate oxidized at 2.5% (PRP-HG-2.5%) to conduct the *in vitro* and *in vivo* studies, since it presented more suitable mechanical properties and degradation profile.

Prior to conduct *in vitro* efficacy studies, *i.e.* proliferation and adhesion studies, we analyzed the biocompatibility of the hydrogels in human fibroblasts (Fig. 3A) and keratinocytes (Fig. 3B). As expected, all tested formulations were cytocompatible, as alginate have excellent biocompatibility [25] and PRP has a human origin.

PRP has extensively proven its beneficial effect in wound healing, promoting the proliferation and migration of cells involved in healing [51]. Hence, we conducted a proliferation study, in order to elucidate whether the actPRP included in the hydrogel formulation was able to maintain its activity (Fig. 3C). As a control for this assay, we used 11% (v/v) of actPRP, which is the same volume of actPRP that was included into the hydrogels, and moreover it is the optimal PRP/media ratio for cell proliferation *in vitro* according to a systematic review by Gentile and Garcovich [52].

Results obtained in fibroblast and keratinocyte human cell lines showed an enhancement in proliferation, thereby highlighting the beneficial effect of actPRP in the formulation developed. In addition, the hydrogel without

PRP (HG-2.5%), was not able to enhance proliferation, pointing out that the proliferation observed in both fibroblast and keratinocytes was due to the effect of soluble factors within the actPRP.

Furthermore, we assessed the cell adhesion ability of the hydrogel to determine if it was able to create a temporary wound matrix substitute. This would provide physical support to enable cell migration and accelerate wound healing [53]. As alginate lacks specific cells adhesion sites, cells did not adhere to the hydrogel composed only of alginate (HG-2.5%), and spare cells without the characteristic fibroblast morphology could be observed on its surface [27]. On the contrary, hydrogels containing actPRP were able to promote cell adhesion, showing a great quantity of cells adhered to its surface with the elongated spindle-shaped fibroblast morphology (Fig. 3D). Such difference between hydrogels could be attributed to the adhesion proteins present in the actPRP — such as fibronectin and fibrin —, which provide ECM-like properties to the formulated composite hydrogel [54].

Results obtained *in vivo* were inconsistent with *in vitro* studies, as the inclusion of actPRP in the hydrogel did not enhance wound healing macroscopically nor microscopically. Hydrogel formulations — PRP-HG-2.5% and HG-2.5% — accelerated wound closure and promoted the maturation of the wound in comparison to control and actPRP alone. However, no differences were found between both groups (Fig. 4). Therefore, we can conclude that the observed effect was solely due to alginate. In fact, the capacity of alginate to enhance wound healing has been previously largely proven, as stated by the variety of commercially available wound care products based on alginate, such as, 3M Tegaderm, Algicell, Algisite, Calcicare, Cutimed alginate, Dermalginate, Kaltostat, Nu-derm *etc.* This healing effect is attributed to the creation of a moist environment at the wound bed, which can reduce wound pain, reduce odor and help in hemostasis [25,55].

As the *in vivo* results were not in line with *in vitro* data, we hypothesized that the lack of effect might be due to the xenogeneic administration of human PRP in mice. To test this hypothesis we conducted *in vitro* cytotoxicity and proliferation studies in mouse fibroblasts (Fig. 5). In contrast to the results obtained with human cells — HDF and HaCaT —, human actPRP was cytotoxic to mouse cells reaching a similar viability to the positive control. In addition, we observed a reduction in cell proliferation, but these results were ascribed to cell death. We did not observe those cytotoxic effects with the hydrogels containing actPRP — PRP-HG and PRP-HG-2.5% —, probably due to the protective effect produced by the sustained release of the soluble factors. Therefore, the deleterious effect of xenogeneic PRP was masked, since the short incubation time of the studies was not enough to release the sufficient amount of soluble factors able to cause cell death. In addition, those hydrogels did not enhance cell proliferation; unlike they did in human cell lines. Hence, the lack of proliferative effect observed in a xenogeneic cell line, might explain the negative results obtained *in vivo*. Results obtained with HG-2.5%, were in agreement with the ones obtained in human cells, as no promotion of proliferation was observed in either of them.

The negative effect of xenogeneic platelets concentrate administration has been already described by Allen et al. using platelet lysate [56]. They observed that a human platelets lysate administration reduced drastically the viability of rat mesenchymal stem cells. They attributed this result to heat-labile proteins present in platelets concentrates. Although, the exact mechanism is not clear, authors point at the complement system, cold agglutinin and antithymocyte globulin as possible causes of the cell death [56–59]. Nevertheless, further investigations are needed in order to elucidate the exact mechanism of the cytotoxicity of xenogeneic PRP.

These results exposed the difficulty in choosing an animal model to conduct studies with human PRP, since the xenogeneic origin could hinder the actual therapeutic effect. Furthermore, the use of animals' autologous or allogeneic PRP also presents a series of limitations. For example, the difficulty to obtain the necessary volume of plasma due to the small size of rodents. In addition, animal blood composition differs from that of humans, leading to PRPs with different properties and efficacy. Moreover, those differences in blood composition could preclude the formation of an adequate platelet concentrate from some animals. For example, a leukocyte-plasma rich

fibrin clot is impossible to produce from rabbit and rat blood [60,61]. Possible solutions to this issue would be to use *ex vivo* human skin models or humanized animal models.

## 5. Conclusion

Overall, the PRP-HG-2.5% formulation showed appropriate characteristics to be used in wound healing, given its rheological/mechanical properties and release of GFs. By oxidizing the alginate we obtained a formulation able to degrade gradually, which could facilitate wound cleaning and avoid the need to remove the dressing, a process that can be harmful for the newly created tissue. In addition, *in vitro* studies conducted in human fibroblasts and keratinocytes highlighted the beneficial effect of actPRP in cell proliferation, a key step in wound healing. Unlike the hydrogel without PRP, it also presented cellular adhesion, which could promote cellular migration into the wound bed by acting as a provisional matrix. Results from the *in vivo* study conducted in diabetic mice (*db/db* mice) were hampered by the deleterious effect of xenogeneic PRP, and hence, only the effect of alginate could be observed. Accordingly, future studies are warranted to evaluate its effectiveness in a reliable preclinical model. To the best of our knowledge, this is the first time a degradable hydrogel composed of oxidized alginate and actPRP has been developed. In addition, as far as we know it is the first time the deleterious effect of xenogeneic PRP has been proven in murine cells.

## Declaration of competing interest

The authors declare that they have no known competing financial interests or personal relationships that could have appeared to influence the work reported in this paper.

## Acknowledgments

I. Garcia-Orue thanks University of the Basque Country (UPV/EHU) for the Dokberri grant (DOCREC19/10). The authors are thankful for the technical and human support provided by SGIker of UPV/EHU. Authors also thank ICTS "NANBIOISIS", specifically the Drug Formulation Unit (U10) of the CIBER in Bioengineering, Biomaterials and Nanomedicine (CIBER-BBN) at the UPV/EHU in Vitoria-Gasteiz. Finally, the authors thank the Open Access funding provided by University of the Basque Country.

## Appendix A. Supplementary data

Supplementary data to this article can be found online at <https://doi.org/10.1016/j.msec.2022.112695>.

## References

- A. Süle, N. Miljković, P. Polidori, S. Kohl, Position paper on an ageing society, *Eur. J. Hosp. Pharm.* 26 (2019) 354–356.
- G. Han, R. Ceilley, Chronic wound healing: a review of current management and treatments, *Adv. Ther.* 34 (2017) 599–610.
- C. Lindholm, R. Searle, Wound management for the 21st century: combining effectiveness and efficiency, *Int. Wound J.* 13 (2016) 5–15.
- H. Brem, O. Stojadinovic, R.F. Diegelmann, H. Entero, B. Lee, I. Pastar, et al., Molecular markers in patients with chronic wounds to guide surgical debridement, *Mol. Med. (Cambridge, Mass.)* 13 (2007) 30–39.
- P.S. Briquez, J.A. Hubbell, M.M. Martino, Extracellular matrix-inspired growth factor delivery systems for skin wound healing, *Adv. Wound Care (New Rochelle)* 4 (2015) 479–489.
- G. Gainza, S. Villullas, J.L. Pedraz, R.M. Hernandez, M. Igartua, Advances in drug delivery systems (DDSs) to release growth factors for wound healing and skin regeneration, *Nanomedicine* 11 (2015) 1551–1573.
- I. Garcia-Orue, J.L. Pedraz, R.M. Hernandez, M. Igartua, Nanotechnology-based delivery systems to release growth factors and other endogenous molecules for chronic wound healing, *J. Drug Deliv. Sci. Technol.* 42 (2017) 2–17.
- A. Lubkowska, B. Dolegowska, G. Banfi, Growth factor content in PRP and their applicability in medicine, *J. Biol. Regul. Homeost. Agents* 26 (2012) 35–225.
- B. De Angelis, M.F.L.M. D'Autilio, F. Orlandi, F. Pepe, S. Garcovich, M.G. Scioli, et al., Wound healing. *In vitro* and *in vivo* evaluation of a bio-functionalized scaffold based on hyaluronic acid and platelet-rich plasma in chronic ulcers, *J. Clin. Med.* 8 (2019) <https://doi.org/10.3390/jcm8091486>.
- S. Giannini, A. Cielo, L. Bonanome, C. Rastelli, C. Derla, F. Corpaci, et al., Comparison between PRP, PRGF and PRF: lights and shadows in three similar but different protocols, *Eur. Rev. Med. Pharmacol. Sci.* 19 (2015) 927.
- P. Heher, S. Mühleder, R. Mittermayr, H. Redl, P. Slezak, Fibrin-based delivery strategies for acute and chronic wound healing, *Adv. Drug Deliv. Rev.* 129 (2018) 134–147.
- S. Lang, M. Loibl, M. Herrmann, Platelet-rich plasma in tissue engineering: hype and Hope, *Eur. Surg. Res.* 59 (2018) 265–275.
- J. Etulain, Platelets in wound healing and regenerative medicine, *Platelets* 29 (2018) 556–568.
- V. Cervelli, I. Bocchini, C. Di Pasquali, B. De Angelis, G. Cervelli, C.B. Curcio, et al., P.R.L. platelet rich lipotransfert: our experience and current state of art in the combined use of fat and PRP, *Biomed. Res. Int.* 2013 (2013), 434191.
- V. Cervelli, L. Lucarini, D. Spallone, L. Palla, G.M. Colicchia, P. Gentile, et al., Use of platelet-rich plasma and hyaluronic acid in the loss of substance with bone exposure, *Adv. Skin Wound Care* 24 (2011) 176–181.
- D. Chouhan, N. Dey, N. Bhardwaj, B.B. Mandal, Emerging and innovative approaches for wound healing and skin regeneration: current status and advances, *Biomaterials* 216 (2019), 119267.
- A. Francesko, P. Petkova, T. Tzanov, Hydrogel dressings for advanced wound management, *Curr. Med. Chem.* 25 (2018) 5782–5797.
- Z. Xu, S. Han, Z. Gu, J. Wu, Advances and impact of antioxidant hydrogel in chronic wound healing, *Adv. Healthc. Mater.* 9 (2020), e1901502.
- D. Eisenbud, H. Hunter, L. Kessler, K. Zulkowski, Hydrogel wound dressings: where do we stand in 2003? *Ostomy Wound Manage* 49 (2003) 52.
- Z. Qian, H. Wang, Y. Bai, Y. Wang, L. Tao, Y. Wei, et al., Improving chronic diabetic wound healing through an injectable and self-healing hydrogel with platelet-rich plasma release, *ACS Appl. Mater. Interfaces* 12 (2020) 55659–55674.
- P.V. Notodihardjo, N. Morimoto, N. Kakudo, M. Matsui, M. Sakamoto, P.H. Liem, et al., Gelatin hydrogel impregnated with platelet-rich plasma releasate promotes angiogenesis and wound healing in murine model, *J. Artif. Organs* 18 (2015) 64–71.
- S. Wei, P. Xu, Z. Yao, X. Cui, X. Lei, L. Li, et al., A composite hydrogel with co-delivery of antimicrobial peptides and platelet-rich plasma to enhance healing of infected wounds in diabetes, *Acta Biomater.* 124 (2021) 205–218.
- P. Zhang, L. Zhou, L. Wang, Q. Dong, A novel nanofiber hydrogel loaded with platelet-rich plasma promotes wound healing through enhancing the survival of fibroblasts, *Med. Sci. Monit.* 25 (2019) 8712–8721.
- M. Qiu, D. Chen, C. Shen, J. Shen, H. Zhao, Y. He, Platelet-rich plasma-loaded Poly(D, L-lactide)-Poly(ethylene glycol)-Poly(D, L-lactide) hydrogel dressing promotes full-thickness skin wound healing in a rodent model, *Int. J. Mol. Sci.* 17 (2016) <https://doi.org/10.3390/ijms17071001>.
- T.G. Sahana, P.D. Rekha, Biopolymers: applications in wound healing and skin tissue engineering, *Mol. Biol. Rep.* 45 (2018) 2857–2867.
- V. Jones, J.E. Grey, K.G. Harding, Abc of wound healing: wound dressings, *BMJ [Br. Med. J.]* 332 (2006) 777–780.
- S. Rekasame, A.R. Boccaccini, Oxidized alginate-based hydrogels for tissue engineering applications: a review, *Biomacromolecules* 19 (2018) 3–21.
- K.H. Bouhadir, K.Y. Lee, E. Alsberg, K.L. Damm, K.W. Anderson, D.J. Mooney, Degradation of partially oxidized alginate and its potential application for tissue engineering, *Biotechnol. Prog.* 17 (2001) 945–950.
- C. Li, R. Fu, C. Yu, Z. Li, H. Guan, D. Hu, et al., Silver nanoparticle/chitosan oligosaccharide/poly(vinyl alcohol) nanofibers as wound dressings: a preclinical study, *Int. J. Nanomedicine* 8 (2013) 4131–4145.
- J. Michaels, S.S. Churgin, K.M. Blechman, M.R. Greives, S. Aarabi, R.D. Galiano, et al., *db/db* mice exhibit severe wound-healing impairments compared with other murine diabetic strains in a silicone-splinted excisional wound model, *Wound Repair Regen.* 15 (2007) 665–670.
- U.K. Sinha, L.A. Gallagher, Effects of steel scalpel, ultrasonic scalpel, CO2 laser, and monopolar and bipolar electrosurgery on wound healing in Guinea pig Oral mucosa, *Laryngoscope* 113 (2003) 228–236.
- R. Cotran, G.K. Kumar, T. Collins, Reparación de los tejidos: proliferacion celular, fibrosis y curación de las heridas, in: R. Cotran, G.K. Kumar, T. Collins (Eds.), *Patología estructural y funcional*, McGraw-Hill, Interamericana, Madrid 2000, pp. 95–120.
- H. Kong, D.J. Mooney, Controlling material properties of ionically cross-linked alginate hydrogels by varying molecular weight distribution, *MRS Proc.* 711 (2001).
- K. Sharun, A.M. Pawde, Variables affecting the potential efficacy of platelet-rich plasma (PRP) in dermatology, *J. Am. Acad. Dermatol.* 84 (1) (2020) E47–E48.
- O.J. Smith, G. Jell, A. Mosahebi, The use of fat grafting and platelet-rich plasma for wound healing: a review of the current evidence, *Int. Wound J.* 16 (2018) 275–285.
- S. Kushida, N. Kakudo, N. Morimoto, T. Hara, T. Ogawa, T. Mitsui, et al., Platelet and growth factor concentrations in activated platelet-rich plasma: a comparison of seven commercial separation systems, *J. Artif. Organs* 17 (2014) 186–192.
- M. Zhang, X. Zhao, Alginate hydrogel dressings for advanced wound management, *Int. J. Biol. Macromol.* 162 (2020) 1414–1428.
- K.A. Kristiansen, H.B. Tomren, B.E. Christensen, Periodate oxidized alginates: depolymerization kinetics, *Carbohydr. Polym.* 86 (2011) 1595–1601.
- X. Kong, L. Chen, B. Li, C. Quan, J. Wu, Applications of oxidized alginate in regenerative medicine, *J. Mater. Chem. B* 9 (2021) 2785–2801.
- A. Gonzalez-Pujana, K.H. Vining, D.K.Y. Zhang, E. Santos-Vizcaino, M. Igartua, R.M. Hernandez, et al., Multifunctional biomimetic hydrogel systems to boost the immunomodulatory potential of mesenchymal stromal cells, *Biomaterials* 257 (2020), 120266.
- M. Virumbrales-Muñoz, E. Santos-Vizcaino, L. Paz, A.M. Gallardo-Moreno, G. Orive, R.M. Hernandez, et al., Force spectroscopy-based simultaneous topographical and mechanical characterization to study polymer-to-polymer interactions in coated alginate microspheres, *Sci. Rep.* 9 (2019) 20112–20114.

- [42] A. Gonzalez-Pujana, A. Rementeria, F.J. Blanco, M. Igartua, J.L. Pedraz, E. Santos-Vizcaino, et al., The role of osmolarity adjusting agents in the regulation of encapsulated cell behavior to provide a safer and more predictable delivery of therapeutics, *Drug Deliv.* 24 (2017) 1654–1666.
- [43] T.B. Lopez-Mendez, E. Santos-Vizcaino, F.J. Blanco, J.L. Pedraz, R.M. Hernandez, G. Orive, Improved control over MSCs behavior within 3D matrices by using different cell loads in both in vitro and in vivo environments, *Int. J. Pharm.* 533 (2017) 62–72.
- [44] I. Batubara, D. Rahayu, K. Mohamad, W.E. Prasetyaningtyas, Leydig cells encapsulation with alginate-chitosan: optimization of microcapsule formation, *J. Encapsul. Adsorpt. Sci.* 2 (2012) 15–20.
- [45] J.L. Wilson, M.A. Najia, R. Saeed, T.C. McDevitt, Alginate encapsulation parameters influence the differentiation of microencapsulated embryonic stem cell aggregates, *Biotechnol. Bioeng.* 111 (2014) 618–631.
- [46] X. Gao, L. Gao, T. Groth, T. Liu, D. He, M. Wang, et al., Fabrication and properties of an injectable sodium alginate/PRP composite hydrogel as a potential cell carrier for cartilage repair, *J. Biomed. Mater. Res. A* 107 (2019) 2076–2087.
- [47] Z. Chen, Y. Hu, J. Li, C. Zhang, F. Gao, X. Ma, et al., A feasible biocompatible hydrogel film embedding Periplaneta Americana extract for acute wound healing, *Int. J. Pharm.* 571 (2019), 118707.
- [48] Y. Tu, M. Zhou, Z. Guo, Y. Li, Y. Hou, D. Wang, et al., Preparation and characterization of thermosensitive artificial skin with a Sandwich structure, *Mater. Lett.* 147 (2015) 4–7.
- [49] M. Matsui, Y. Tabata, Enhanced angiogenesis by multiple release of platelet-rich plasma contents and basic fibroblast growth factor from gelatin hydrogels, *Acta Biomater.* 8 (2012) 1792–1801.
- [50] E. Kobayashi, L. Fluckiger, M. Fujioka-Kobayashi, K. Sawada, A. Sculean, B. Schaller, et al., Comparative release of growth factors from PRP, PRF, and advanced-PRF, *Clin. Oral Investig.* 20 (2016) 2353–2360.
- [51] P. Samadi, M. Sheykhasan, H.M. Khoshnani, The use of platelet-rich plasma in aesthetic and regenerative medicine: a comprehensive review, *Aesthet. Plast. Surg.* 43 (2018) 803–814.
- [52] P. Gentile, S. Garcovich, Systematic review—the potential implications of different platelet-rich plasma (PRP) concentrations in regenerative medicine for tissue repair, *Int. J. Mol. Sci.* 21 (2020) <https://doi.org/10.3390/ijms21165702>.
- [53] I. Negut, G. Dorcioman, V. Grumezescu, Scaffolds for wound healing applications, *Polymers* 12 (2020) 2010.
- [54] E. Jooybar, M.J. Abdekhoodaie, M. Alvi, A. Mousavi, M. Karperien, P.J. Dijkstra, An injectable platelet lysate-hyaluronic acid hydrogel supports cellular activities and induces chondrogenesis of encapsulated mesenchymal stem cells, *Acta Biomater.* 83 (2019) 233–244.
- [55] D. Yang, K.S. Jones, Effect of alginate on innate immune activation of macrophages, *J. Biomed. Mater. Res.* 90A (2009) 411–418.
- [56] A.B. Allen, E.B. Butts, I.B. Copland, H.Y. Stevens, R.E. Guldberg, Human platelet lysate supplementation of mesenchymal stromal cell delivery: issues of xenogenicity and species variability, *J. Tissue Eng. Regen. Med.* 11 (2017) 2876–2884.
- [57] A. Salama, B. Göttsche, V. Vaidya, S. Santos, C. Mueller-Eckhardt, Complement-independent lysis of human red blood cells by cold hemagglutinins, *Vox Sang.* 55 (1988) 21–25.
- [58] M.S. Zand, T. Vo, J. Huggins, R. Felgar, J. Liesveld, T. Pellegrin, et al., Polyclonal rabbit antithymocyte globulin triggers B-cell and plasma cell apoptosis by multiple pathways, *Transplantation* 79 (2005) 1507–1515.
- [59] D.A. Rubenstein, W. Yin, Platelet-activation mechanisms and vascular remodeling, *Compr. Physiol.* (2018) 1117–1156.
- [60] A. Simonpieri, M. Del Corso, A. Vervelle, F. Inchingolo, G. Sammartino, D.M. Dohan Ehrenfest, et al., Current knowledge and perspectives for the use of platelet-rich plasma (PRP) and platelet-rich fibrin (PRF) in oral and maxillofacial surgery: part 2: bone graft, implant and reconstructive surgery, *Curr. Pharm. Biotechnol.* 13 (2012).
- [61] D.M. Dohan Ehrenfest, N. Lemo, R. Jimbo, G. Sammartino, Selecting a relevant animal model for testing the in vivo effects of Choukroun's platelet-rich fibrin (PRF): Rabbit tricks and traps, *Oral Surg. Oral Med. Oral Pathol. Oral Radiol. Endod.* 110 (2010) 413–416.